

## Inverse Hook Method for Measuring Oscillator Strengths

W. A. van Wijngaarden, K. Bonin, W. Happer, E. Miron,<sup>(a)</sup> D. Schreiber,<sup>(b)</sup> and T. Arisawa<sup>(c)</sup>

*Department of Physics, Princeton University, Princeton, New Jersey 08544*

(Received 15 October 1985)

We describe a new method for measuring oscillator strengths for transitions between excited atomic states. The oscillator strength is determined from changes in the angular distribution or polarization of fluorescent light induced by the ac Stark effect of a laser pulse. The method can be thought of as a variant of the hook method in which the roles of atoms and photons have been interchanged.

PACS numbers: 32.70.Cs, 32.80.-t

Oscillator strengths for optical transitions in atoms and molecules are notoriously difficult to determine.<sup>1-3</sup> In this paper we describe an effective new method to measure absolute oscillator strengths for transitions between excited states.

The essence of the method is illustrated in Fig. 1. An atomic state (*a*) with electronic angular momentum  $J = \frac{3}{2}$  is anisotropically populated by excitation with polarized light, as shown in Fig. 1(a). A pulse of laser light (the light-shift pulse), off resonant by an amount  $\Delta\nu$  from the resonant frequency for transition to a *second* state of interest (*b*), is appropriately polarized to cause virtual transitions to and from the second state shown in Fig. 1(b) and thereby transfer atoms between the sublevels of the *populated* state (*a*). At the end of the laser pulse the sublevel populations have been modified as shown in Fig. 1(c). The resulting changes in sublevel population can be monitored by observation of changes in the angular distribution or polarization of fluorescent light from the populated state. The oscillator strength for transitions between the populated and second state can thereby be determined as we discussed below.

The virtual transitions of Fig. 1 can be described with the light-shift operator  $H$ , defined by its matrix elements between sublevels  $i$  and  $j$  of the populated state<sup>4,5</sup>:

$$H_{ij} = - \sum_k \epsilon \cdot \mathbf{D}_{ik} \mathbf{D}_{kj} \cdot \epsilon^* / h \Delta\nu. \quad (1)$$

Here  $\Delta\nu = \nu - \nu_0$  is the frequency detuning of the laser

frequency  $\nu$  from the resonant frequency  $\nu_0$ , the classical electric field of the light is  $\mathbf{E} = \epsilon e^{-i\omega t} + \epsilon^* e^{i\omega t}$ , and the electric dipole moment operator of the transition is  $\mathbf{D}$ . The sum extends over all sublevels  $k$  of the second state. If the second state lies higher than the populated state, rather than lower as is assumed in Fig. 1, the sign is changed in the right-hand side of (1) and the amplitudes  $\epsilon$  and  $\epsilon^*$  are interchanged. The evolution caused by the light-shift pulse is described by the unitary time-evolution operator

$$U = \exp\left[-(i/\hbar) \int_0^T H dt\right] \\ = \sum_m |m\rangle \langle m| e^{-i\phi(m)}, \quad (2)$$

where the time integral extends over the pulse duration  $T$ , and  $|m\rangle$  are the eigenstates of  $H$ , i.e.,  $H|m\rangle = E(m)|m\rangle$ . For linearly polarized light,  $m$  is the azimuthal quantum number for an axis along  $\epsilon$ , and the phase angles are given by

$$\phi(m) = \hbar^{-1} \int_0^T E(m) dt \\ = (3r_e \lambda / 2h) C^2 (J_b 1 J_a; m 0) (f_{ab} F / \Delta\nu). \quad (3)$$

Here  $r_e = 2.82 \times 10^{-13}$  cm is the classical electron radius,  $\lambda$  is the optical wavelength of the transition,  $C$  is a Clebsch-Gordan coefficient,<sup>6</sup> the laser-pulse fluence is  $F = (c/2\pi) \int_0^T |\epsilon|^2 dt$ , and the electronic angular momenta of the populated and second states are  $J_a$  and  $J_b$ .

The oscillator strength is defined by

$$f_{ab} = [2(E_b - E_a) / 3r_e c^2 \hbar^2 (2J_a + 1)] \sum_{m, \mu} \langle J_a m | \mathbf{D} | J_b \mu \rangle \cdot \langle J_b \mu | \mathbf{D} | J_a m \rangle, \quad (4)$$

where we use the convention of Corney.<sup>7</sup> Here  $E_a$  and  $E_b$  are the energies of the populated and second states. The fluence  $I$  of linearly polarized fluorescent light emitted by the atoms after the light-shift pulse has passed is given by<sup>8</sup>

$$I = A [1 + B P_2(\cos\theta) \langle T_{20} \rangle_f], \quad (5)$$

where the constant  $A$  accounts for detector efficiency.  $P_2(\cos\theta)$  is the second Legendre polynomial, where  $\theta$  is the angle between the  $z$  axis (vertical axis) and the polarization direction of detected linearly polarized

fluorescence. The population imbalances in the populated state are conveniently described by the mean alignment  $\langle T_{20} \rangle$ , where for a state with angular momentum  $J = \frac{3}{2}$ ,  $T_{20} = \frac{1}{2} J_z^2 - \frac{5}{8}$ . The *final* ( $f$ ) alignment after the passage of the light-shift pulse is denoted by  $\langle T_{20} \rangle_f$ . The coefficient<sup>8</sup>  $B$  in (5) equals  $-2$  if fluorescence is observed for a transition from a populated state having  $J_a = \frac{3}{2}$  to a terminal state with  $J_c = \frac{1}{2}$ . If  $J_c = \frac{3}{2}$ , then  $B = \frac{8}{5}$ .

We assume pure alignment of the populated state

before the light-shift pulse, as shown in Fig. 1(a). The light-shift pulse will then transform the initial alignment  $\langle T_{20} \rangle_i$  into a final alignment  $\langle T_{20} \rangle_f$  as follows:

$$\langle T_{20} \rangle_f = \langle T_{20} \rangle_i \text{Tr}(UT_{20}U^\dagger T_{20}) = \langle T_{20} \rangle_i [1 + \frac{3}{4} \sin^2\beta(3 \sin^2\beta - 4)(1 - \cos\Delta\phi)], \quad (6)$$

where the light-shift pulse is linearly polarized at an angle  $\beta$  to the  $z$  axis and the phase difference is given in terms of the phases (3) by

$$\Delta\phi = \phi(\pm \frac{3}{2}) - \phi(\pm \frac{1}{2}) = F/\Delta F_0, \quad (7)$$

where

$$1/\Delta F_0 = \sum_b \alpha_{ab} f_{ab} [1/\lambda - 1/\lambda_{ab}]^{-1}. \quad (8)$$

Here the sum extends over the two second states,  $5^2P_{1/2}$  and  $5^2P_{3/2}$ , which significantly affect these experiments. The coefficients  $\alpha_{ab}$  are readily calculated from (3) to be  $\alpha_{ab} = (4r_e/5hc)\lambda_{ab}$  if  $J_b = \frac{3}{2}$  and  $\alpha_{ab} = -r_e\lambda_{ab}/hc$  if  $J_b = \frac{1}{2}$ . To derive the last term of (6) it is convenient to use the matrix representation of  $T_{20}$  on the basis  $|m\rangle$  discussed in connection with (2).

Because of spatial nonuniformities of the light-shift pulse, different atoms experience different fluences and therefore different phase angles (3). Perhaps the simplest fluence distribution to consider, which was closely approximated in our experiment, is the exponential distribution with mean fluence  $F_0$ ,

$$P(F) = (1/F_0) \exp(-F/F_0), \quad (9)$$

characteristic of a fully developed speckle pattern.<sup>9</sup> The spatially averaged value of the fluence-dependent part of the signal is then easily shown to be

$$\langle \cos\Delta\phi \rangle = \int_0^\infty P(F) dF \cos\Delta\phi = (\Delta F_0)^2 / [(\Delta F_0)^2 + F_0^2]. \quad (10)$$

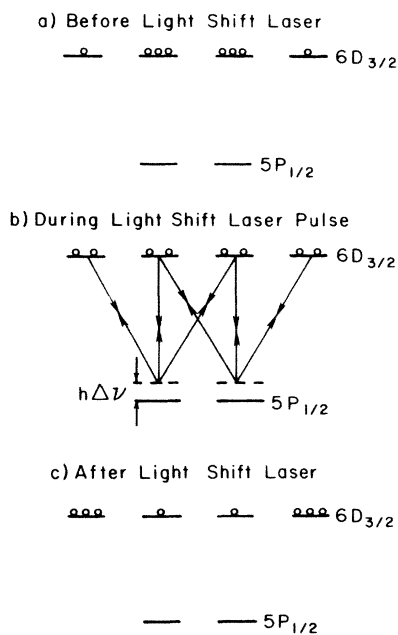


FIG. 1. Redistribution of populations of Zeeman sublevels by the light-shift pulse.

Although the fluence distribution measured in our experiments is similar to (9), model calculations show that the interpretation of the parameter  $|\Delta F_0|$  as the half width of a depolarization curve remains valid to within a few percent for many plausible fluence distributions, such as broad Gaussian, square-pulse, and triangular-pulse distributions.

A diagram of our apparatus to measure oscillator strengths is shown in Fig. 2. A Pyrex-glass sample cell contains a small amount of  $^{85}\text{Rb}$  metal. The cell is heated to  $120^\circ\text{C}$  to provide a Rb number density of about  $2 \times 10^{13} \text{ cm}^{-3}$ . Two dye lasers are pumped by a doubled Nd:YAG (neodymium-doped yttrium aluminum garnet) laser at a 20-Hz repetition rate. The 4-nsec output pulses are delayed with respect to each other by about 15 nsec by path-length differences from the lasers to the sample cell. The first pulse at  $6969 \text{ \AA}$  drives a two-photon transition from the  $5S_{1/2}$  ground state of Rb to the  $6D_{3/2}$  excited state, which has a radiative lifetime of about 250 nsec. The propagation direction of the exciting pulse is taken as the  $y$  axis of a coordinate system (see Fig. 2). The laser is polarized along the  $z$  (vertical) axis, the direction of a 14-G magnetic field which is used to decouple the nuclear

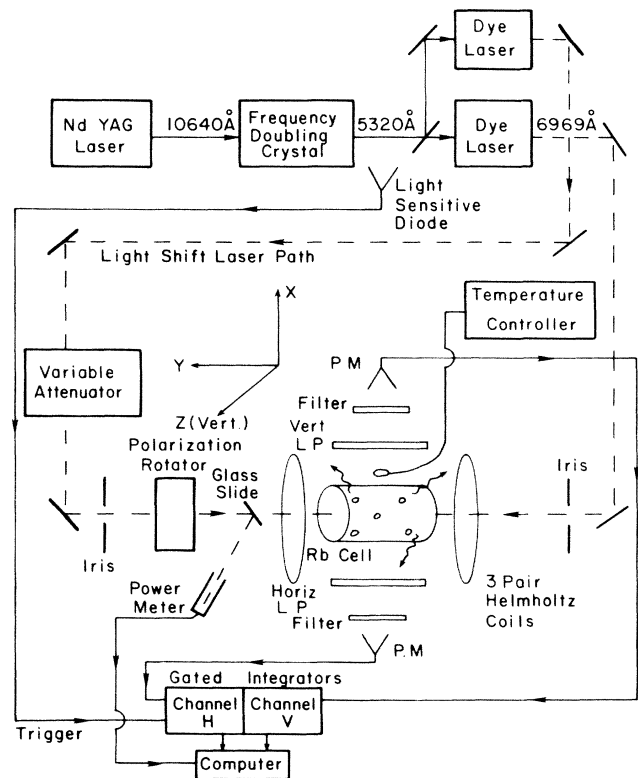


FIG. 2. Experimental apparatus.

and electronic spin polarizations in the excited state.<sup>8</sup> The magnetic field is not big enough to substantially alter the excited-state evolution described by (2) during the 4-nsec interval of the light-shift pulse. The two-photon excitation produces an initial population distribution similar to that of Fig. 1(a). The two-photon transition can only populate the sublevels with  $m = \pm \frac{1}{2}$  directly and the relatively small population of the  $\pm \frac{3}{2}$  sublevels, which we always observe in our experiments, is probably due to parasitic lasing at  $12\mu$  on the very strong transitions  $6D \rightarrow 7P$ .

Some 15 nsec later a pulse of 6206-Å light, propagating along the  $y$  axis, causes transitions like those sketched in Fig. 1(b). This light-shift pulse is linearly polarized at the "magic angle"  $\beta = 54.7^\circ$  to the  $z$  axis in order to maximize the fluence-dependent term in (6).

Fluorescent light was detected along the  $x$  axis as shown in Fig. 2. In each channel, detected light first passed through a linear polarizer and was then directed through an interference filter (20-Å bandwidth) before finally being focused onto a photomultiplier. The signals from the two channels after the light-shift pulse are integrated for 400 nsec with gated integrators, and the ratio of the vertical to horizontal signals is calculated in a small computer and accumulated as a function of the fluence for each laser shot. By taking ratios we are able to eliminate the effect of shot-to-shot intensity fluctuations (about 20%) of the exciting laser pulses. The fluence of the light-shift pulse is measured for each shot by the sampling of a small fraction of each light-shift pulse with a calibrated laser-energy meter. Both the exciting and light-shift laser beams are aligned to pass through two circular irises located one on each side of the cell. From the measured pulse energy  $E$  and iris area  $A = 0.20 \text{ cm}^2$  we determine the mean fluence  $F_0 = E/A$  of the light-shift pulse.

The laser detuning is fixed by pressurizing of the oscillator cavity with up to 1 atm of Freon. To determine accurately the relationship between pressure and detuning, Freon is leaked out of the cavity. The change in laser wavelength is monitored by counting interference fringes produced by an etalon while simultaneously determining the Rb resonance frequency from the optogalvanic signal of a Rb lamp.<sup>10</sup>

Actual data for the transition  $6D_{3/2} \rightarrow 5P_{1/2}$  discussed above and for the analogous transition  $6D_{3/2} \rightarrow 5P_{3/2}$  for which the wavelengths of the second laser and the fluorescent light were interchanged are shown in Fig. 3. The measured ratio  $V/H$  has a fluence-dependent part which is well represented by a Lorentzian curve as predicted by (10). Also, the signs of the depolarization curves are opposite, in accordance with the different signs of  $B$  in (5). Using the two oscillator strengths  $f_{ab}$  for transitions to the  $5^2P_{1/2}$  and  $5^2P_{3/2}$  states as free parameters, we fit the theoret-

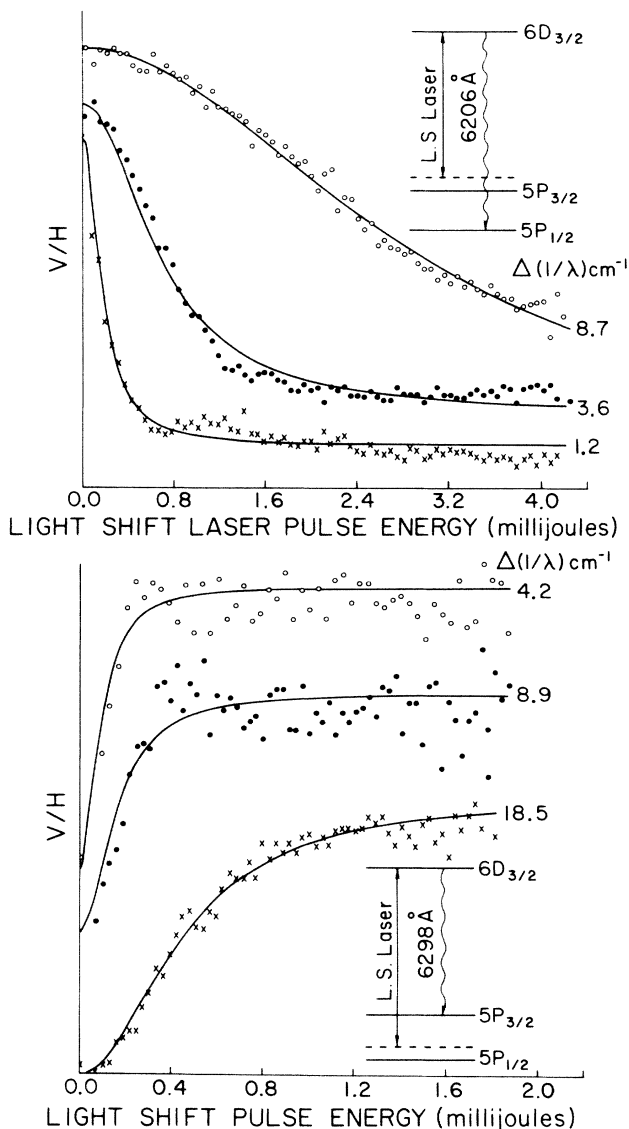


FIG. 3. Curves of the fluorescent polarization vs light-shift-pulse energy for various detunings  $\Delta(1/\lambda)$ . Light-shift laser wavelengths are indicated by solid lines, while detected fluorescence transitions are represented by wiggly lines.

ical curve (8) to the experimentally determined half widths of Fig. 3, which are interpreted as the absolute values of the parameter  $\Delta F_0$ , in accordance with the discussion of Eq. (10). An example is shown in Fig. 4. Our measurements for several transitions in rubidium are compared in Table I to Coulomb-approximation calculations and to values already in the literature.

Huber<sup>1</sup> has reviewed other schemes to measure oscillator strengths by the dynamic Stark shift or the optical Autler-Townes effect. Although the method described here makes use of the same physical phenomenon, as evidenced by our use of the light-shift operator (1) as the starting point of the analysis, this method is unique in its combination of light-shift

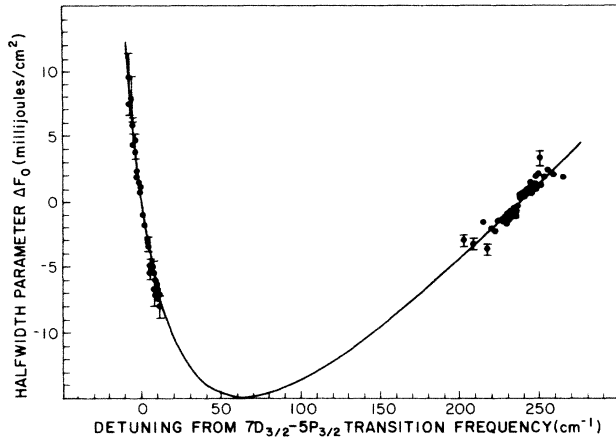


FIG. 4. Comparison of theory (solid line) from (9) with experimental data. We have set  $|\Delta F_0|$  equal to the widths of curves similar to those in Fig. 3 obtained for the  $7D_{3/2}$ - $5P$  transitions. The sign of  $\Delta F_0$  was chosen to agree with that predicted by (8).

effects with perturbed angular correlations. The atoms "integrate" the light shift and respond to the pulsed laser fluence in much the same way that a ballistic galvanometer responds to the total charge of a current pulse. The temporal substructure of the laser pulse is not important. Unlike methods based on absorption or curves of growth, where the relative amounts of Doppler, collisional, and natural broadening are crucial, this method uses light which is detuned so far off resonance that details of the line shape are not important. With this method it is possible to measure directly oscillator strengths of transitions out of any state for which radiative lifetimes can be determined by pulsed laser excitation and fluorescent monitoring. There is no need to measure branching ratios. Oscillator strengths can be determined for transitions to lower or higher states, including autoionizing states.

In conclusion we point out a close connection between this method and the classical hook method<sup>1-3</sup> for measuring oscillator strengths. In the hook method an interferometer is used to measure the optical phase-retardation angle  $\phi_h$  produced by an atomic vapor of number density  $N$  and length  $l$ . The phase retardations of the vapor and reference paths in the conventional hook method correspond to the  $2J_a + 1$  atomic phase angles of (3). The hook phase shift is related to the atomic phase shifts of (3) by

$$(F/h\nu)\phi_n = Nl\bar{\phi},$$

where the mean atomic phase shift is

$$\bar{\phi} = (2J_a + 1)^{-1} \sum_m \phi(m).$$

The quantity  $Nl$  is the atomic column density (atoms per unit area) and the quantity  $F/h\nu$  is the photon column density (photons per unit area). In short, our method is basically an inverse hook method where we

TABLE I. Oscillator strengths of rubidium.

$b$	$a$	This expt.	$f_{ba}$ Theory <sup>a</sup>	Goltz <i>et al.</i> <sup>b</sup>
$5P_{1/2}$	$6D_{3/2}$	0.027(5)	0.036	0.030
$5P_{3/2}$	$6D_{3/2}$	0.0026(t)	0.0040	0.0032
$5P_{1/2}$	$7D_{3/2}$	0.021(4)	0.024	0.020
$5P_{3/2}$	$7D_{3/2}$	0.0018(4)	0.0026	0.0020

<sup>a</sup>Reference 11.

<sup>b</sup>Reference 12.

have interchanged the role of atoms and photons. We do this because pulsed lasers provide adequate and easily measured photon column densities (i.e., fluences). Only enough excited atoms are needed to give a good fluorescent signal. It is often impossible to obtain adequate excited-atom column densities and, more importantly, to measure such densities to permit absolute oscillator strengths to be determined by the conventional hook method.

This work was supported by Lawrence Livermore National Laboratory Subcontract No. 3181505. We are grateful to W. Liao for his help with computer simulations, to S. Lavi, R. Miles, and J. Christenson for technical assistance, and finally to R. Solarz and J. Paisner for initial and continued encouragement. One of us (W.v.W.) would like to thank the Canadian National Research Council for their financial support.

(a) Present address: Nuclear Research Centre-Negev, Beer-Sheva, Israel.

(b) Present address: AT&T Bell Laboratory, Whippany, N.J. 07981.

(c) Present address: Japan Atomic Energy Research Institute, Tokai Research Establishment, Ibaraki-Ken, Japan.

<sup>1</sup>M. C. E. Huber and R. J. Sandeman, *Phys. Scr.* **22**, 373 (1980).

<sup>2</sup>W. L. Wiese, in *Progress in Atomic Spectroscopy: Part B*, edited by W. Hanle and H. Kleinpoppen (Plenum, New York, 1979), Vol. 1.

<sup>3</sup>E. W. Foster, *Rep. Prog. Phys.* **27**, 469 (1964).

<sup>4</sup>J. P. Barrat and C. Cohen-Tannoudji, *J. Phys. Radium* **22**, 329, 443 (1961).

<sup>5</sup>W. Happer and B. S. Mathur, *Phys. Rev.* **163**, 12 (1967).

<sup>6</sup>M. E. Rose, *Elementary Theory of Angular Momentum* (Wiley, New York, 1957).

<sup>7</sup>A. Corney, *Atomic and Laser Spectroscopy* (Clarendon, Oxford, 1977).

<sup>8</sup>The complete expression for  $I$  has a term of the form  $\sum_m \langle T_{2m} \rangle Y_{2m}^*(\theta, \pi/2)/(1 + i\omega m \tau)$ . We neglect the contributions from terms with  $m \neq 0$  because  $\omega \tau = 25$  in our experiments. For a description of the fluorescent light in terms of spherical tensors see, for example, R. Gupta, S. Chang, and W. Happer, *Phys. Rev. A* **6**, 529 (1972).

<sup>9</sup>J. C. Dainty, *Laser Speckle* (Springer, New York, 1975).

<sup>10</sup>E. Miron, I. Smilanski, J. Liran, S. Lavi, and G. Erez, *IEEE J. Quantum Electron.* **15**, 194 (1979).

<sup>11</sup>D. R. Bates and A. Damgaard, *Philos. Trans. Roy. Soc. London* **242**, 101 (1949).

<sup>12</sup>D. von der Goltz, W. Hansen, and J. Richter, *Phys. Scr.* **30**, 244-248 (1984).